Magnetohydrodynamic mixed convection effects on the removal process of fluid particles from an open cavity in a horizontal channel

Rouhollah Yadollahi Farsani [*1], Behzad Ghasemi[2], Saiied Mostafa Aminossadati[3]

[1]*Associate Lecturer, Ardal Center, Shahrekord branch, Islamic Azad University, Shahrekord, Iran*
[2]*Chemical Engineering Professor, Engineering Faculty, Shahrekord University, Shahrekord, Iran*
[3]*Senior Lecturer, School of Mechanical and Mining Engineering, the University of Queensland, QLD 4072, Australia*

A B S T R A C T

This paper presents the results of a numerical study on the heat transfer performance and the removal process of fluid particles under the influence of magnetohydrodynamic mixed convection in a horizontal channel with an open cavity. The bottom wall of the cavity is heated at a constant temperature (T_h) while the top wall of the channel is maintained at a relatively low temperature (T_c). Air with a uniform velocity (u_0) and temperature (T_c) is introduced to the channel. The analysis is carried out for a range of values of the Grashof number ($10^3 \leq Gr \leq 10^6$), the Reynolds number ($1 \leq Re \leq 100$), and the Hartmann number ($0 \leq Ha \leq 100$).The results show that the heat transfer rate increases as the Grashof number increases and decreases as the Reynolds and Hartmann numbers increase. It is also shown that the removal process accelerates as the Grashof number increases and, however, decelerates as the Reynolds and Hartmann numbers increase.

1. Introduction

The accumulation of contaminant substances of the working fluid in the channels with open cavities is crucial for the performance of equipment in chemical and food processing plants. The increased pressure losses, the reduced heat transfer rate and the adverse hygiene conditions are some of the results of this accumulation. The removal of the fluid particles from the open cavity depends on the flow field characteristics and the geometry of the channels and cavities[1]. In many situations, the flow within the open cavity is influenced by the convective heat transfer. Any change of convection flow parameters can significantly affect the process of contaminant removal[2]. The results of studies on the hydrodynamic mixed convection flow in channels with open cavities show that the flow field within the cavity can considerably be affected by the characteristics of the mixed convection flow[3-7].

The study of mixed convection of electrically-conducting fluids in the magnetohydrodynamic (MHD) devices such as coolers of nuclear reactors, thermal insulators, and micro-electronic devices should account for the effect of a transverse magnetic field on the fluid flow and the heat transfer mechanisms. It has been found that the fluid flow experiences the Lorentz force due to the influence of the magnetic field. There has been an increasing interest to understanding of the magnetohydrodynamic convective heat transfer of electrically-conducting fluids in cavities, [8-11]. The common finding of all these studies is that the magnetic field can suppress the convective flow field within the cavity and that the magnetic field is one of the important factors in the examination of the thermal performance of the cavity.

The effect of a magnetic field on the flow behavior and the heat transfer performance of channels has beenextensively studied and documented in the literature,[12-16].Mahmud et al. [17]analytically

Corresponding author: Rouhollah Yadollahi Farsani , Associate Lecturer, Ardal Center, Shahrekord branch, Islamic Azad University, Shahrekord, Iran. Tel/Fax: +98-382-6224041,
Email: r.yadollahi@iaushk.ac.ir

analyzed the thermodynamics of mixed convection in a channel that was under the influence of transverse magnetohydrodynamic effects. They numerically calculated the average entropy generation number for channels with different aspect ratios. They also proposed a correlation between a geometric parameter and the minimum irreversibility at a particular ratio of the Grashof number to the Reynolds number and a particular value of the Hartmann number. RaveendraNath et al [18] examined the magnetohydrodynamic mixed convective heat and mass transfer through a porous medium in a non-uniformly heated vertical channel with heat sources and dissipation. They analyzed the velocity, temperature, shear stress, and the rate of heat transfer for different variations of the governing parameters, and observed the dissipative effects on the flow, heat, and mass transfer.Rahman et al [19] numerically examined the magnetohydrodynamic mixed convection in a horizontal channel with an open cavity. They presented their results in terms of the streamlines, the isotherms, the average Nusselt number, the drag force, and the average bulk temperature. Their results indicated that the flow and temperature fields within the cavity were strongly affected by the variations of the Rayleigh, Reynolds, and Hartmann numbers.

In addition to earlier studies on the mixed convection of magnetohydrodynamic flows in channels with an open cavity, the focus of the current study is to examine the effects of the magnetic field on the laminar mixed convection flow in the channel and the dynamic removal of fluid particles from the cavity. The simulation is carried out for a range of values of the Grashof number ($10^3 \leq Gr \leq 10^6$), the Reynolds number ($1 \leq \text{Re} \leq 100$), and the Hartmann number ($0 \leq Ha \leq 100$). The results are presented in terms of the streamlines, the isotherms, and the average Nusselt number at the steady state condition, and the transient removal process of fluid particles from the cavity.

2. Problem Definition

The geometry considered in this study is a two-dimensional horizontal channel with an open cavity (Fig. 1). The length of the cavity (L) is considered as the reference length in the dimensional analysis. The length of the channel is $8L$. The cavity is located at a distance of $3L$ from the entrance of the channel. The height of the inflow and outflow openings is equal to the depth of the cavity ($L/2$). Air with a uniform velocity (u_o) and temperature (T_c) is introduced to the channel. The flow is assumed to be laminar and incompressible with the Prandtl number of Pr=0.71. The radiation effects are assumed to be negligible. The bottom wall of the cavity
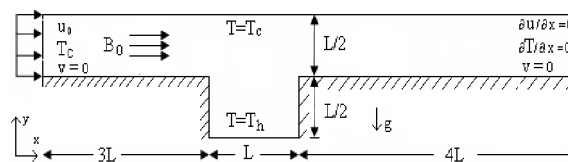

Fig.1 Schematic diagram of the problem

is heated at a constant temperature (T_h) while the top wall of the channel is maintained at a relatively low temperature (T_c). The bottom wall of the channel and the vertical walls of the cavity are thermally insulated. A uniform magnetic field with the strength of B_o is applied in the same direction of the channel. All the thermophysical properties of the air flow are assumed constant except for the variation in density with temperature, where a Boussinesq approximation is applied. Fully-developed conditions are considered at the exit section of the channel and the no-slip boundary condition (U=V=0) are assumed on the walls. The analysis is carried out for different lengths of the channel exit section to ensure that the fully-developed condition at the exit of the channel is an appropriate boundary condition.

3. Governing Equations

The nature of the magnetohydrodynamic flows includes both fluid dynamics (Navier–Stokes) and electrodynamics (Maxwell) equations. Lorentz force and Ohm's law have been considered in these equations. The Ohm's law is taken into consideration and the magnetic Reynolds number of the flow is taken to be small so that the flow induced distortion of the applied magnetic field can be neglected. The additional field induced by the fluid motion is weak compared with the applied field. The dimensionless form of continuity, momentum, and energy equations describing the flow under the Boussinesq approximation are as following:

$$\frac{\partial U}{\partial X} + \frac{\partial V}{\partial Y} = 0 \tag{1}$$

$$\frac{\partial U}{\partial \tau} + U\frac{\partial U}{\partial X} + V\frac{\partial U}{\partial Y} = -\frac{\partial P}{\partial X} + \frac{1}{\text{Re}}(\frac{\partial^2 U}{\partial X^2} + \frac{\partial^2 U}{\partial Y^2}) \tag{2}$$

$$\frac{\partial V}{\partial \tau} + U\frac{\partial V}{\partial X} + V\frac{\partial V}{\partial Y} = -\frac{\partial P}{\partial Y} + \frac{1}{\text{Re}}(\frac{\partial^2 V}{\partial X^2} + \frac{\partial^2 V}{\partial Y^2}) + \frac{Gr}{\text{Re}^2}\theta - \frac{Ha^2}{\text{Re}}V \tag{3}$$

$$\frac{\partial \theta}{\partial \tau} + U\frac{\partial \theta}{\partial X} + V\frac{\partial \theta}{\partial Y} = \frac{1}{Re\,Pr}(\frac{\partial^2 \theta}{\partial X^2} + \frac{\partial^2 \theta}{\partial Y^2}) \tag{4}$$

In the above equations, the following dimensionless parameters are used:

$$X = \frac{x}{L}, \quad Y = \frac{y}{L}, \quad U = \frac{u}{u_O}, \quad V = \frac{v}{u_O}, \quad P = \frac{\bar{p}}{\rho\, u_O^2}$$

$$Ha = B_o\, L \sqrt{\frac{\sigma}{\rho\, v}}, \quad \theta = \frac{T - T_c}{T_h - T_c}, \quad Re = \frac{\rho\, u_O\, L}{v}, \quad (5)$$

$$Pr = \frac{v}{\alpha}, \quad \tau = \frac{u_o\, t}{L}, \quad Gr = \frac{g\, \beta\, (T_h - T_c) L^3}{v^2}$$

The term on the right-hand side of Eq. (3) includes the Lorentz force induced by the interaction of the magnetic field and the convective motion. The boundary conditions for the present problem are specified as following:

inlet	$U = 1,\ V = 0,\ \theta = 0,$
outlet (Fully	$\partial U / \partial X = 0,\ V = 0,$
developed condition)	$\partial \theta / \partial X = 0$
top wall	$U = 0,\ V = 0,\ \theta = 0$
other walls	$U = 0,\ V = 0,\ \partial \theta / \partial N = 0$
cavity's bottom	$U = V = 0,\ \theta = 1$

(6)

where N is the dimensionless distances in both X and Y directions acting normal to the surface. The local Nusselt number at the heated surface is calculated by $Nu = -\partial \theta / \partial Y$. Therefore, the average Nusselt number is obtained by integrating the Nusselt number over the cavity's bottom wall:

$$Nu_m = -(1/L) \int_0^L \partial \theta / \partial Y\, dx \qquad (7)$$

4. Numerical Method of Solution

The governing equations presented in Eqs. (1)-(4) along with the boundary conditions (Eq. (6)) are numerically solved by employing the finite volume method and using the staggered grid arrangement. The power law scheme, which is a combination of the central difference and the upwind schemes, is used to discrete the convection terms, "Patankar et al (1980)". A staggered grid system, in which the velocity components are stored midway between the scalar storage locations, is used. The solution of the fully-coupled discretized equations is obtained iteratively using the TDMA method. In order to get the accurate solutions, the error limit of 10^{-6} is considered as the convergence condition.

The process of hydrodynamic removal of fluid particles from the cavity is carried out by using Marker and Cell (MAC) method of "Harlow and Welch (1965)". In every time step, the displacement of marker cell k (x_k,

y_k) is determined after solving the velocity and pressure field by using the following equations:

$$X_k^{n+1} = U_k^{n+1} \Delta\tau + X_k^n, \quad Y_k^{n+1} = V_k^{n+1} \Delta\tau + Y_k^n \qquad (8)$$

where U_k is the horizontal velocity at the marker position (X_k), and X_k^{n+1} is the new position of marker k. The velocity components at the marker positions are calculated by a weighted interpolation of velocities in surrounding cells as described by "McKee et al. (2008)". Passive markers are used to visualize the flow patterns and to quantify the hydrodynamic removal markers from the cavity.

5. Grid Independence and Code Validation

The grid independence test is performed for $Gr=10^3$ and $Ha =50$ and at different values of the Reynolds number. Table 1 shows the dependence of the Nusselt number on the grid size. The results show that a grid size of 420×60 is adequate to ensure the grid independency. The time step independence test is also performed at $Gr=10^3$, $Ha =50$, and $Re=100$. The percentage of markers removed from the cavity as the time progresses for various values of the time step is given in Fig. 2.

The $d\tau = 0.0025$ is selected which results in a highly accurate solution. The present code is validated against the results of "Leong et al. (2005)" for the mixed convection heat transfer in a channel with an open cavity. Table 2 shows the average Nusselt number for $Gr=10^3$ and different values of the Reynolds number. This comparison indicates a good agreement between the two numerical results.

6. Results and Discussions

The results of the numerical analysis of the magnetohydrodynamic mixed convection in the channel with an open cavity for a range of values of the Grashof number ($10^3 \leq Gr \leq 10^6$), the Reynolds number ($1 \leq Re \leq 100$) and the Hartmann number ($0 \leq Ha \leq 100$) are presented. First, the flow and temperature fields and the heat transfer performance of the channel for a steady-state process are examined. Then, the results of the transient removal process of fluid particles from the cav.

6.1 Steady-State Thermal Performance

In this section, the influence of the Hartmann number

Table 1: Average Nusselt number for Ha=50 and Gr = 10^3

Grid	20×200	40×280	60×390	60×420	70×430	70×450
Re=1	1.79	1.87	2.08	2.19	2.23	2.26
Re=10	2.22	2.32	2.35	2.41	2.42	2.42
Re=100	2.37	2.51	2.65	2.91	2.98	3.07

(Ha=0, 50, 100) on the flow and temperature fields for Gr=10^6 and three various values of the Reynolds number (Re=1, 10, 100) are presented. Fig. 3 illustrates the streamlines and isotherms for Re=1, where the buoyancy effects dominate the flow field in the channel and the heat transfer is mainly due to the natural convection. In the absence of the magnetic field (Ha=0), strong buoyancy-induced flow circulations are evident in the cavity. These circulations are also extended into the channel and in the direction of the mainstream flow. When the magnetic field is applied to the channel, the flow circulations become weaker and do not follow the mainstream flow anymore. The opposite effects of the magnetic field and buoyancy forces can be seen in the equation 3. The isotherms show thin thermal boundary layers in the vicinity of the cavity's bottom wall for Ha=0. As the Hartmann number increases, the isotherms distribute more uniformly between the bottom wall of the cavity and the top wall of the channel.

Fig. 4 shows the streamlines and isotherms for $Re = 10$, where the contribution of the forced convection in the flow and temperature fields increases. Three circulating cells are evident inside and outside of the cavity for all values of the Hartmann number. The small circulating cell at the bottom of the cavity grows as the Hartmann number increases. The isotherms distribution is also affected by the effect of the magnetic field. Less concentration of the isotherms near the bottom wall of the cavity is observed as the Hartmann number increases.
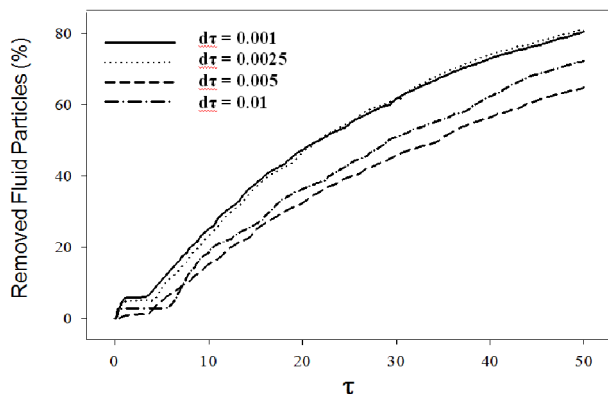

Fig.2 Time step independence study at Re=100, Gr=10^3, and Ha=50

Table 2: Validation of the current study against the results of Leong et al. (2005) for $Gr = 10^3$ and $Pr = 0.71$

Re	1	10	100	1000
Nu$_m$ " Leong et al. (2005)"	1.45	1.70	2.25	5.15
Nu$_m$ [present]	1.41	1.75	2.40	5.32
Error [%]	2.70	2.90	6.66	3.33

Fig. 5 shows the streamlines and isotherms for Re=100, where the forced convection dominates the flow and temperature fields. In the absence of the magnetic field, a large circulating cell is observed that covers the entire cavity. As the Hartmann number increases, the strength of the circulating cell decreases due to the effect of the magnetic field while the mainstream flow in the channel remains unaffected. The density of stratified isotherms near the bottom wall of the cavity decreases as the Hartmann number increases. This is also observed for Re=1 and 10.

It has been observed that for all values of the Reynolds number, the intensity of isotherms in the vicinity of the cavity's bottom wall decreases as the Hartmann number increases. This suggests lower heat transfer rates for the cavity as the strength of the
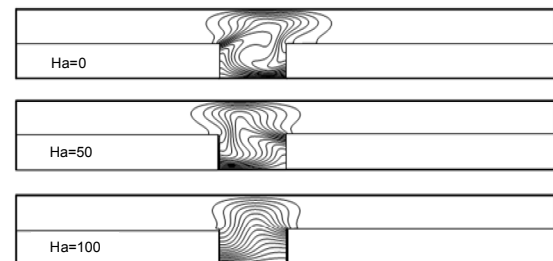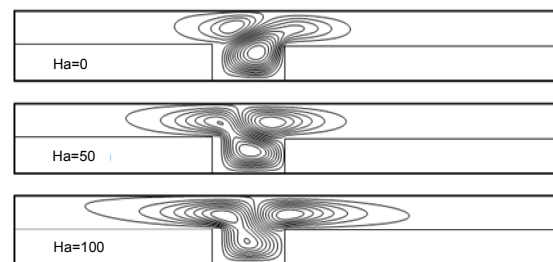

Fig.3 Streamlines (top) and isotherms (bottom) (Steady-state, Re=1, and Gr=10^6)
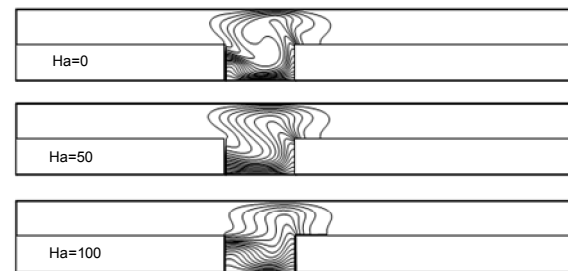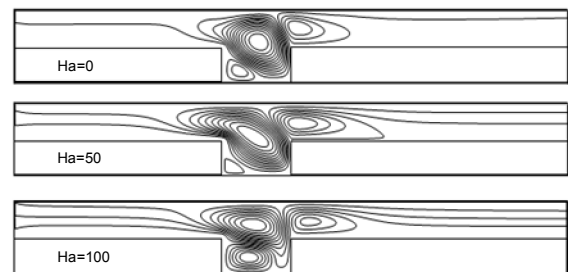

Fig.4 Streamlines (top) and isotherms (bottom) (Steady-state, Re=10, and Gr=10^6)

magnetic field increases. In order to examine the cavity's heat transfer performance, the values of the average Nusselt number (Nu_m) at different Hartmann, Reynolds, and Grashof numbers are presented in Fig. 6. The results show that for all values of the Reynolds number, the average Nusselt number increases as the Grashof number increases. This is due to the influence of strengthened buoyancy effects on the heat transfer process as the Grashof number increases. An extreme increase can be observed in Nusselt number at $Gr=10^6$ and $Re=100$. This is due to the strong cell that is generated in the cavity as showed in fig.5. This cell plays a major role in free convective heat transfer from the bottom of the cavity to the main stream.

The results also show that for all values of the Reynolds and Grashof numbers, the average Nusselt number decreases as the Hartmann number increases. This is due to the influence of the magnetic field on the flow and temperature fields within the cavity. The influence of the magnetic field on reducing the heat transfer rate is more evident at higher values of the Grashof number, where the buoyancy-induced flow dominates the heat transfer mechanism. This can be clearly explained by Eq. 3 in which the buoyancy term appears as a source term and the magnet term appears as a sink term. It is important to mention that by increasing the Re number, the forced convection dominates the heat transfer mechanism and the effect of Hartmann number decreases (see Fig. 6). It is also evident that the average Nusselt number decreases as the Reynolds number increases. This can be clearly explained by cavity circulating cells at the higher Reynolds numbers in Fig. 5.

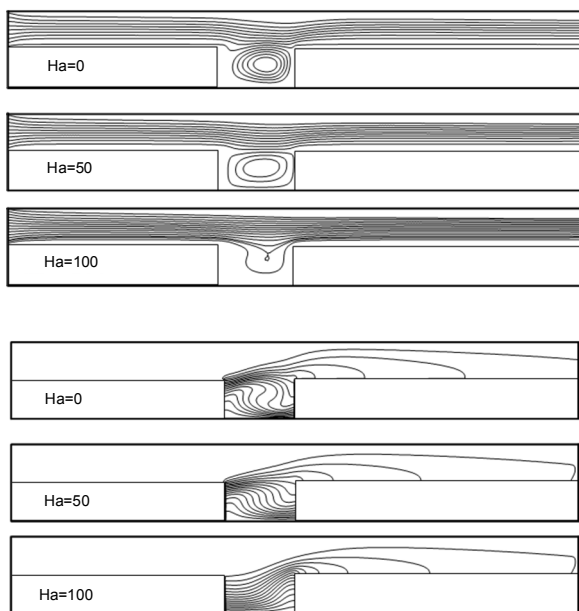*6.2 Transient Removal of Fluid Particles from the Cavity*

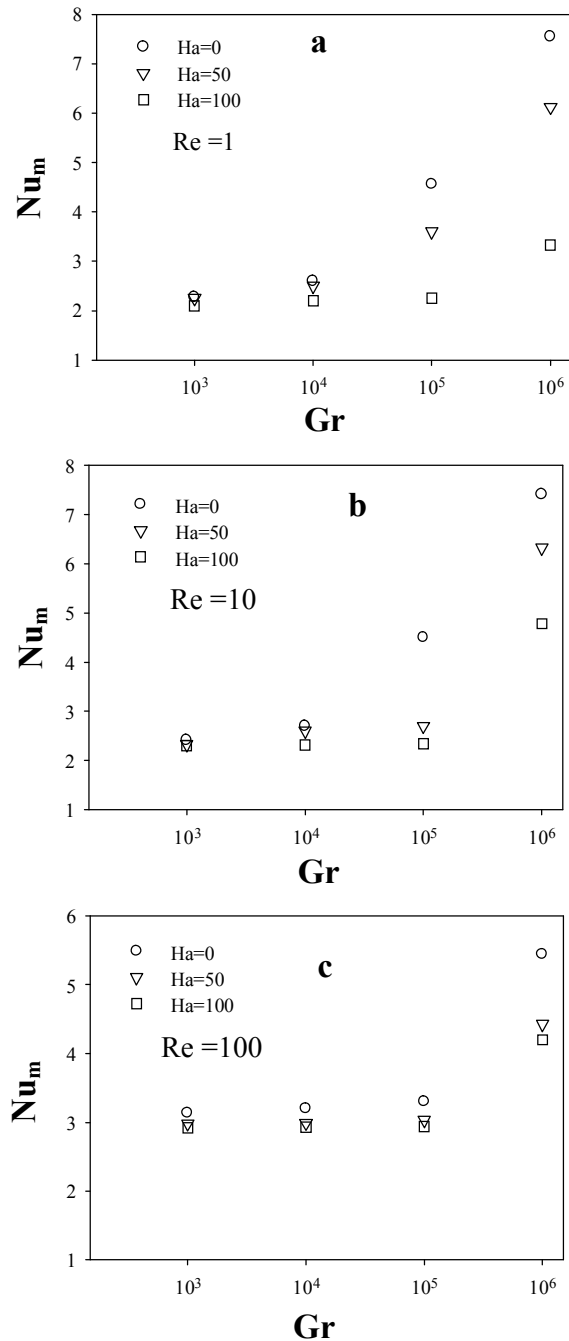Fig.5 Streamlines (top) and isotherms (bottom) (Steady-state, Re=100, and Gr=10^6)

Fig.6 Variation of the average Nusselt number with Hartman and Grashof numbers (Steady-state process) (a) Re=1 (b) Re=10 (c) Re=100

In this section, the removal process of fluid particles from the cavity at different values of the Grashof, Reynolds, and Hartmann numbers is examined. Here, $U=0$, $V=0$, and $\theta=0$ are considered as the initial values at $\tau=0$. The removal process of the fluid particles from the cavity at dfferent times ($\tau=0,10,20$) is illustrated in Fig. 7a-b for $Gr=10^6$ and $Gr=10^3$, respectively. The Reynolds and Hartmann numbers are considered to be $Re=100$ and $Ha=50$, respectively. For this exercise, 2000 fluid particles are introduced in the cavity prior to initiating the flow. The results show that for both values of the

Grashof number, the removal process is set in motion and the amount of fluid particles removed from the cavity is increased as the time passes. The path-line of the fluid particles that enter the channel downstream of the cavity follows the streamlines observed in Fig. 5. It can also be observed that as the Grashof number increases from $Gr=10^6$ to $Gr=10^3$, the rate of particleremoval from the cavity increases due to the stronger buoyancy force.

Fig. 8 shows the time history of the removal process of fluid particles for different values of the Grashof, Reynolds, and Hartmann numbers. As mentioned earlier, 2000 fluid particles are considered in the cavity prior to initiating the flow. Fig. 8-a shows the time history of the removal process of the fluid particles at various values of the Grashof number ($Gr=10^3$, 10^5, 10^6). Here, the Reynolds and Hartmann numbers are $Re=100$ and $Ha=50$, respectively. The results show that the percentage of the removed particles increases with time for all values of the Grashof number. The results also show that the percentage of the removed particles increases as the Grashof number increases. This is due to the strengthening of the buoyancy forces that direct the particles out of the cavity.

Fig. 8-b shows the time history of the removal process of the fluid particles at various values of the Reynolds number ($Re=1$, 10, 100). Here, the Grashof and Hartmann numbers are $Gr=10^6$ and $Ha=50$, respectively. The results show that at low Reynolds numbers ($Re=1$ and $Re=10$), the percentage of removed particles increases rapidly and reaches 100%. This is due to the dominant effect of the buoyant flow within the cavity with respect to the mainstream flow through the channel. At higher values of the Reynolds number ($Re=100$), a slow process of removal is observed and 20% of the fluid particles are still left within the cavity in the timeframe considered in the analysis.

This happens because the mainstream flow through the channel is much stronger than the buoyant flow within the cavity, and prevents the particles to be removed from the cavity (see Fig. 5).

Fig. 8-c presents the time history of the removal process of the fluid particles at various values of the Hartmann number ($Ha=0$, 50, 100). Here, the Reynolds and Grashof numbers are $Re=100$ and $Gr=10^6$, respectively. The results show that in the absence of the magnetic field, the fluid particles are able to move out of the cavity very rapidly. However, as the force of the magnetic field increases, the removal process decelerates. The results also show that the slowest removal process corresponds to $Ha=50$ amongst the values considered for the Hartmann number. The reason for this is that the natural convection plays the key role in removing the fluid particles from the cavity at $Ha=50$ while the forced convection is the main drive for the removal process at $Ha=100$. Therefore, it can be said that an accurate investigation of the removal process of the fluid particles from the cavity needs a simultaneous examination of the effects of the magnetic field, the buoyant flow in the cavity, and the forced convection in the channel.

7. Conclusions

The heat transfer performance as well as the removal process of fluid particles under the influence of magnetohydrodynamic mixed convection in a horizontal channel with an open cavity is numerically examined. The steady-state streamlines, isotherms, and heat transfer rate, and the transient removal process of fluid particles from the cavity at various Grashof, Reynolds, and Hartmann numbers are examined. The results of the numerical analysis have led to the following conclusions:

The steady-state flow and temperature fields within the cavity are influenced by the variations of the Grashof, Reynolds, and Hartmann numbers. In general, the buoyancy-induced flow circulations that are generated in the cavity are weakened, and their extension into the channel is limited as the magnetic field is applied. For all values of the Reynolds number, the intensity of isotherms in the vicinity of the cavity's bottom wall
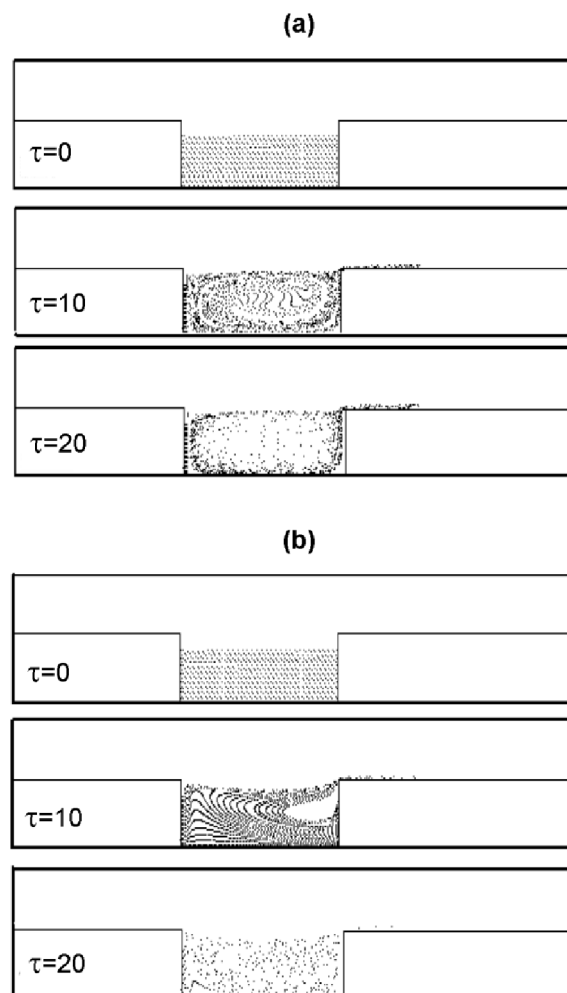

Fig.7 Removed fluid particles from cavity at different times (Re =100, Ha=50)
(a) Gr=10^6 (b) Gr=10^3

decreases as the Hartmann number increases. This can be considered as an indication of less heat transfer due to the influence of the magnetic field.

In order to understand the steady-state thermal behavior of the channel, the average Nusselt number at various Grashof, Reynolds, and Hartmann numbers is examined. The results show that the heat transfer rate increases as the Grashof number increases due to the stronger buoyant flow field. The heat transfer rate, however, decreases as the Reynolds number increases due to the impact of the mainstream flow in the channel on the buoyancy-driven flow circulations within the cavity. The heat transfer rate also decreases as the Hartmann number increases due to the negative influence of the magnetic field on the flow field in the cavity.

The transient removal process of fluid particles from the cavity is also influenced by the variations of the

Grashof, Reynolds, and Hartmann numbers. In general, the removal process accelerates as the Grashof number increases due to the stronger buoyant flow circulations and their influence on directing the fluid particles out of the cavity. The removal process, however, decelerates at high values of the Reynolds number due to the limitations caused by the mainstream flow on the flow field within the cavity. In addition, the rate of removed fluid particles from the cavity is generally reduced due to the influence of the magnetic field.

Nomenclature

B_o	Magnetic field strength
C_p	Specific heat, $J/kg.K$
$d\tau$	Dimensionless time Step
g	Gravitational acceleration (m/s^2)
Gr	Grashof number, $g\beta(T_h - T_c)L^3/v^2$
Ha	Hartmann number, $B_0L\sqrt{\sigma/\rho v}$
L	Cavity width (m)
N	Normal vector to the surface
Nu	Nusselt number, $Nu = -(\partial\theta/\partial N)$
Nu_m	Average Nusselt number, $Nu_m = -(1/L)\int \partial\theta/\partial Y$
p	Fluid pressure, Pa
$\bar{p}$	Modified pressure, $p + \rho_o gy$
P	Dimensionless pressure, $\bar{p}/\rho u_o^2$
Re	Reynolds number, $\rho u_0 L/\mu$
Pr	Prandtl number, v/α
t	Time (s)
T	Temperature ($^\circ C$)
u_o	Inlet flow velocity (m/s)
u	x-component of velocity (m/s)
U	Dimensionless velocity in x direction (u/u_o)
v	y-component of velocity (m/s)
V	Dimensionless velocity in y direction (v/u_o)
x, y	Coordinates
X, Y	Dimensionless coordinates, $x/L, y/L$
Greek	
α	Thermal diffusivity (m2s-1), $\kappa/\rho c_p$
β	Coefficient of Thermal expansion (K^{-1})
τ	Coefficient of Solutal expansion (K^{-1})
σ	Electrical conductivity, $\mu S/cm$
μ	Dynamic viscosity (Nsm-2)
v	Kinematic viscosity (m2s-1), μ/ρ
θ	Angular direction
ρ	Density (kg/m3)
ψ	Stream function

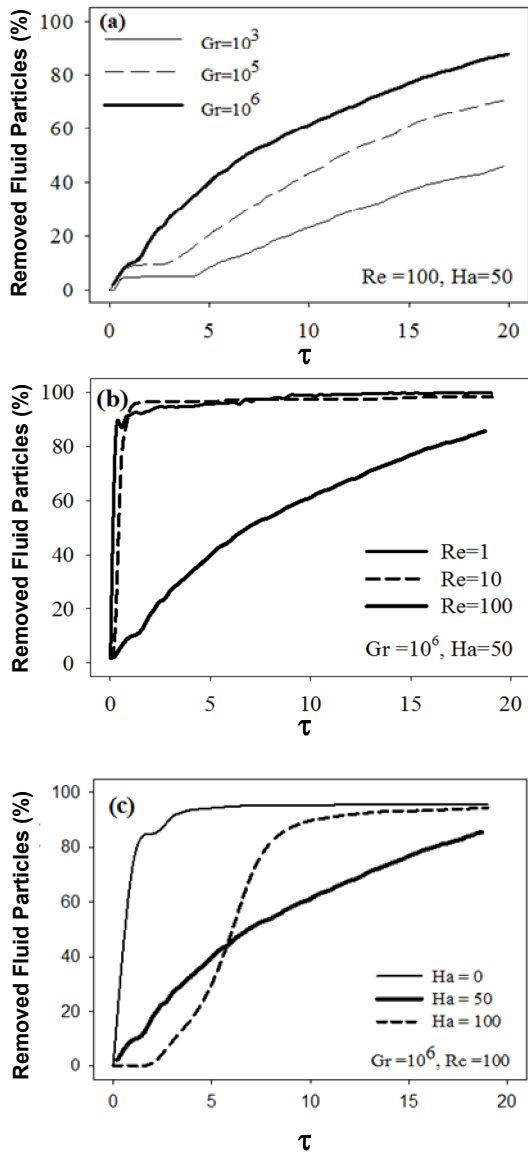Fig.8 Time history of removal process at various values of Grashof, Reynolds, and Hartmann numbers

Superscript

c	*Cold wall*
h	*Hot wall*
m	*Average*
o	*Entry condition*

References

[1]. L. C.Fang, "Effect of mixed convection on transient hydrodynamic removal of a contaminant from a cavity," International Journal of Heat and Mass Transfer, 46(11) 2039-2049, (2003).

[2]. L. C.Fang, "Effect of duct velocity profile and buoyancy-induced flow on efficiency of transient hydrodynamic removal of a contaminant from a cavity," International Journal for Numerical Methods in Fluids, 44(12),1389-1404, (2004).

[3]. N. M.Brown, and F. C.Lai, "Correlations for combined heat and mass transfer from an open cavity in a horizontal channel," International Communications in Heat and Mass Transfer, 32(8),1000-1008, (2005).

[4]. B. Premachandran, and C.Balaji, "Mixed convection heat transfer from a horizontal channel with protruding heat sources," Heat and Mass Transfer/Waerme- und Stoffuebertragung, 41(6), 510-518, (2005).

[5]. I. A.Ermolaev, and A. I.Zhbanov, "Mixed convection in a horizontal channel with local heating from below," Fluid Dynamics, 39(1) 29-35,(2004).

[6]. J. C.Leong, N. M.Brown, and F. C.Lai, "Mixed convection from an open cavity in a horizontal channel," International Communications in Heat and Mass Transfer, 32(5), 583-592, (2005).

[7]. S. M. Aminossadati, and B. Ghasemi, "A numerical study of mixed convection in a horizontal channel with a discrete heat source in an open cavity," European Journal of Mechanics, B/Fluids, 28(4), 590-598,(2009).

[8]. J. P.Garandet, T.Alboussiere, and R.Moreau, "Buoyancy driven convection in a rectangular enclosure with a transverse magnetic field," International Journal of Heat and Mass Transfer, 35(4), 741-748,(1992).

[9]. S. Alchaar, P.Vasseur, and E.Bilgen, "Natural convection heat transfer in a rectangular enclosure with a transverse magnetic field," Journal of Heat Transfer, 117(3), 668-673,(1995).

[10]. N.Rudraiah, R. M. Barron, M.Venkatachalappa, and C. K.Subbaraya, "Effect of a magnetic field on free convection in a rectangular enclosure," International Journal of Engineering Science, 33(8), 1075-1084, (1995).

[11]. B.Ghasemi, S. M.Aminossadati, and A.Raisi, "Magnetic field effect on natural convection in a nanofluid-filled square enclosure," International Journal of Thermal Sciences, 50(9), 1748-1756,(2011).

[12]. R.Siegel, "Effect of magnetic field on forced convection heat transfer in a parallel plate channel," Journal of Applied Mechanics, 25, 415-16, (1987).

[13]. L. H. Back, "Laminar heat transfer in electrically conducting fluids flowing in parallel plate channels," International Journal of Heat and Mass Transfer, 11(11), 1621-1636,(1968).

[14]. R. A. Alpher, "Heat transfer in magnetohydrodynamic flow between parallel plates," International Journal of Heat and Mass Transfer, 3(2),108-112,(1961).

[15]. T.Sawada, T.Tanahashi, and T.Ando, "Two-dimensional flow of magnetic fluid between two parallel plates," Journal of Magnetism and Magnetic Materials, 65(2), 327-329,(1987)

[16]. H. A.Attia, "Transient MHD flow and heat transfer between two parallel plates with temperature dependent viscosity," Mechanics Research Communications, 26(1), 115-121,(1999).

[17]. S.Mahmud, S. H.Tasnim, and M. A. H. Mamun, "Thermodynamic analysis of mixed convection in a channel with transverse hydromagnetic effect," International Journal of Thermal Sciences, 42(8), 731-740, (2003).

[18]. P.R. Nath, P. M. V.Prasad, and D. R. V.PrasadaRao, "Computational hydromagnetic mixed convective heat and mass transfer through a porous medium in a non-uniformly heated vertical channel with heat sources and dissipation," Computers and Mathematics with Applications, 59(2), 803-811, (2010).

[19]. M. M.Rahman, S.Parvin, R.Saidur, and N. A.Rahim, "Magnetohydrodynamic mixed convection in a horizontal channel with an open cavity," International Communications in Heat and Mass Transfer, 38(2), 184-193, (2011).

[20]. S. V. Patankar, "Numerical heat transfer and fluid flow," Hemisphere Publishing Corporation, Taylor and Francis Group, New York, 113-137, (1980).

[21]. S. McKee, M. F.Tome, V. G. Ferreira, J. A.Cuminato, A.Castelo, F. S.Sousa, and N.Mangiavacchi, "THE MAC method," Computers and Fluids, 37, 907-930, (2008).

[22]. F. H. Harlow, and J. E.Welch, "Numerical calculation of time-dependent viscous incompressible flow of fluid with free surface," Physics of Fluids, 8(12), 2182-2189, (1965).